Erratum: Searching for $(\gamma, \alpha)/(\gamma, n)$ branching points in the γ-process path near $A = 100$ [Phys. Rev. C 101, 015801 (2020)]

R. Kelmar, A. Simon, O. Olivas-Gomez, P. Millican, C. S. Reingold, E. Churchman, A. M. Clark,
S. L. Henderson, S. E. Kelly, D. Robertson, E. Stech, and W. P. Tan

We have discovered that the energy loss in the targets that were used was underestimated. This means that the $E_{c.m.}$ at the center of the targets given in the paper were too high by 100–200 keV. So the χ^2 calculations were redone using the corrected energy loss and $E_{c.m.}$. We found that although the individual best-fit models were different, the overall model that best fit the whole region was unchanged.

Although the best-fit models were not the same for three of the four reactions measured, the new best-fit model and the old best-fit model differ by less than 50% across the energy range that was measured. The ^{108,110}Cd(α, γ) ^{112,114}Sn new and old best-fit models agree within 1% below the opening of the neutron separation channel. Also, the recommended model still
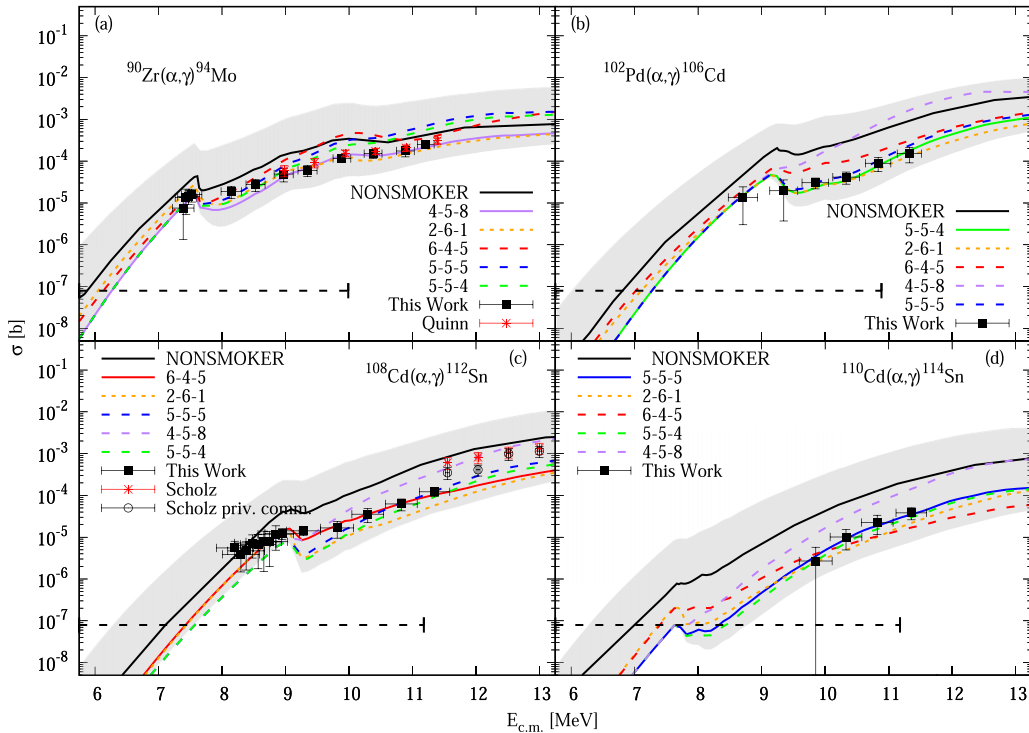

FIG. 3. Cross-section measurements for (a) ^{90}Zr(α,γ) ^{94}Mo, (b) ^{102}Pd(α,γ) ^{106}Cd, (c) ^{108}Cd(α,γ) ^{112}Sn, and (d) ^{110}Cd(α,γ) ^{114}Sn obtained in this paper (solid squares), literature values (asterisks) [1,2], and unpublished work (open circles) [3]. In the combinations of three numbers the first number corresponds to a level-density model, the second number is an α-optical model potential, and the third number is a γ-strength function model available in TALYS. The models that these refer to are described in the text. The gray shaded area indicates the range of cross sections predicted by different combinations of TALYS parameters. The solid black line shows the prediction from the NONSMOKER code. The solid colored line shows the TALYS calculations for the parameter combination that gives the best fit to the data for the individual reaction. The yellow line shows the TALYS calculations for the parameter combination 2-6-1, that gives the best fit for all of the reactions. The long dashed lines show the TALYS calculations for the parameter combinations that give the best fit for the other reactions measured. The black dashed line indicates the Gamow window for the reaction.
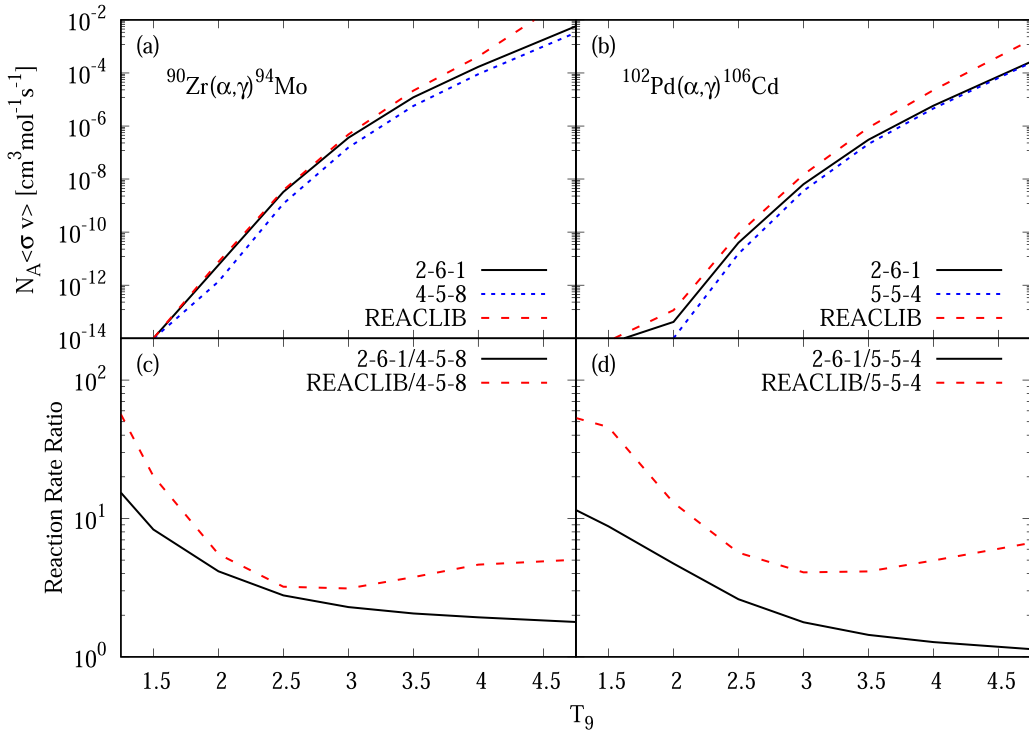
FIG. 4. (a) Reaction rates for ^{90}Zr(α,γ) ^{94}Mo. The blue (short dashed) line shows the TALYS combination that provided the best fit for the measured cross sections. The black (solid) line shows the reaction rate from the recommended TALYS combination. The red (dashed) line shows the rate given by the REACLIB database. (b) Reaction rates for ^{102}Pd(α,γ) ^{106}Cd. The blue (short dashed) line shows the TALYS combination that provided the best fit for the measured cross sections. The black (solid) line shows the reaction rate from the recommended TALYS combination. The red (dashed) line shows the rate given by the REACLIB database. (c) The ratios of the recommended model combination to the best-fit model combination (black, solid) line as well as the ratio of the REACLIB model to the best-fit model (red, dashed) line for the ^{90}Zr(α,γ) ^{94}Mo reaction. (d) The ratios of the recommended model combination to the best-fit model combination (black, solid) line as well as the ratio of the REACLIB model to the best-fit model (red, dashed) line for the ^{102}Pd(α,γ) ^{106}Cd reaction. The numbers in the legends refer to the LD-αOMP-γSF models used in the TALYS calculations.

reproduces all of the cross-section measurements within a factor of 2, which is a large improvement over the factor of 10 that is achieved by the NONSMOKER model.

In addition, the recommended reaction rate is still within a factor of 10 of the best-fit rate for all of the reactions over the temperature range of interest. In all cases the recommended rate is still an improvement upon the rates given in the REACLIB database.

As the overall recommended model for the whole region was unaffected, the conclusions of the paper are unchanged.

Figures 3–6 were affected by these changes, and the updated figures are shown below. In addition, Tables II–IV were updated and are below.

The following parts of the text were also affected. All figures and table numbers correspond to the original text.

(1) The last two sentences of the second to last paragraph on p. 3 should read: This uncertainty generally accounted for less than 20% of the total uncertainty except for the data points at lower energies where there was a steep change in the cross section. In those cases this uncertainty added, at most, 55% to the uncertainty.

(2) The last sentence of the last paragraph on p. 3 should read: The beam resolution from the tandem pelletron has an uncertainty of 1 to 2 keV, the beam energy definition's uncertainty was estimated to be up to 20 keV, and the energy loss through the targets ranged between 100 and 300 keV.

(3) The first full paragraph on p. 7 should read: The parameter combination that was found to best fit each reaction individually is plotted as a solid colored line in Fig. 3. For the ^{90}Zr(α,γ) ^{94}Mo cross-section data the χ^2 value for each combination was calculated with respect to the data in this paper as well as the previous measurements from Quinn et al. [1]. From this, the parameter combination 4-5-8 was determined to provide the best description for the ^{90}Zr(α,γ) ^{94}Mo data. The best-fit model to the ^{102}Pd(α,γ) ^{106}Cd cross-section values given in this paper is the combination 5-5-4. The best-fit model to the ^{108}Cd(α,γ) ^{112}Sn cross-section values given in this paper is the combination 6-4-5. Due to the large discrepancy between the ^{108}Cd(α,γ) ^{112}Sn results given in this paper and the previous measurements of this reaction,

TABLE II. Measured cross-section values for the four (α,γ) reactions. The $E_{c.m.}$ reported is the energy at the center of the target.

$E_{c.m.}$ (MeV)	σ (μb)	$E_{c.m.}$ (MeV)	σ (μb)
		^{90}Zr	
11.21(13)	253(50)	8.53(15)	27.4(8.6)
10.89(14)	175(48)	8.14(16)	18.9(6.1)
10.38(14)	151(34)	7.52(16)	15.9(5.4)
9.89(14)	116(24)	7.47(17)	14.3(5.2)
9.35(15)	61(18)	7.434(17)	13.4(8.1)
8.97(15)	49(17)	7.39(17)	7.5(6.2)
		^{102}Pd	
11.33(19)	151(60)	9.85(21)	30.5(8.8)
10.83(20)	89(33)	9.35(22)	19(16)
10.33(21)	41(13)	8.71(23)	14(11)
		^{108}Cd	
11.35(24)	122(28)	8.75(28)	7.8(5.9)
10.82(25)	62(20)	8.66(28)	7.7(6.2)
10.30(25)	35(13)	8.57(28)	6.8(5.0)
9.81(26)	16.7(7.2)	8.48(28)	7.3(4.1)
9.28(27)	14.2(3.2)	8.38(29)	4.7(3.0)
8.95(27)	12.4(3.5)	8.30(29)	3.9(2.4)
8.85(28)	11.8(6.9)	8.20(29)	5.5(2.5)
		^{110}Cd	
11.36(24)	38(12)	10.33(25)	10.1(5.1)
10.82(25)	23(11)	9.85(26)	2.7(3.0)
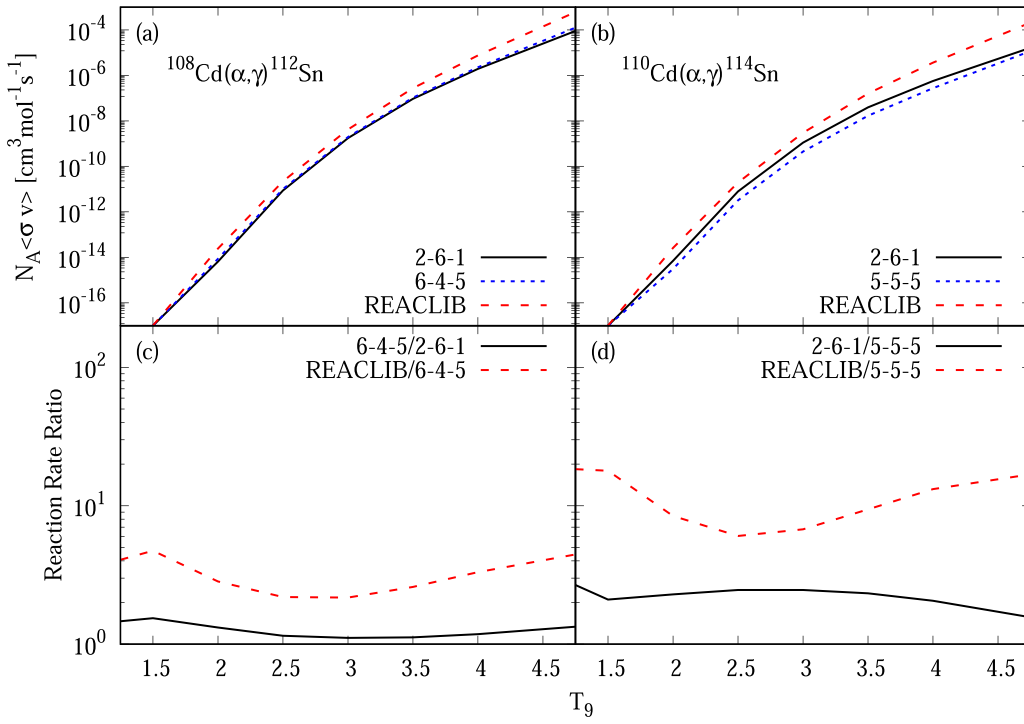
FIG. 5. (a) Reaction rates for ^{108}Cd(α,γ) ^{112}Sn. The blue (short dashed) line shows the TALYS combination that provided the best fit for the measured cross sections. The black (solid) line shows the reaction rate from the recommended TALYS combination. The red (dashed) line shows the rate given by the REACLIB database. (b) Reaction rates for ^{110}Cd(α,γ) ^{114}Sn. The blue (short dashed) line shows the TALYS combination the provided the best fit for the reaction. The black (solid) line shows the reaction rate from the recommended TALYS combination. The red (dashed) line shows the rate given by the REACLIB database. (c) The ratios of the recommended model combination to the best-fit model combination (black, solid) line as well as the ratio of the REACLIB model to the best-fit model (red, dashed) line for the ^{108}Cd(α,γ) ^{112}Sn reaction. (d) The ratios of the recommended model combination to the best-fit model combination (black, solid) line as well as the ratio of the REACLIB model to the best-fit model (red, dashed) line for the ^{110}Cd(α,γ) ^{114}Sn reaction. The numbers in the legends refer to the LD-αOMP-γSF models used in TALYS calculations.
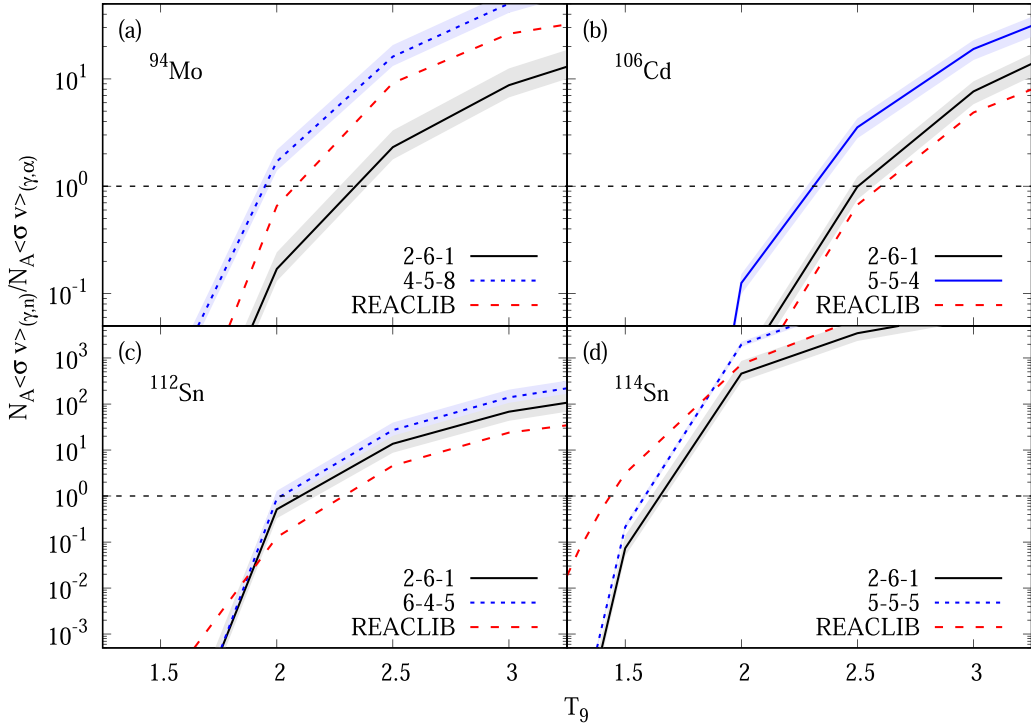
FIG. 6. Ratios of the (γ, n) reaction rates to the (γ, α) reaction rates for (a) ^{94}Mo, (b) ^{106}Cd, (c) ^{112}Sn, and (d) ^{114}Sn. The red (long dashed) line give the rates from the REACLIB database, the blue (short dashed) line gives the (γ, n) and (γ, α) rates calculated in TALYS using the model combination that best fits the individual reaction, and the black (solid) line is the (γ, n) and (γ, α) rates calculated in TALYS using recommended reaction rates. The black dashed line indicates the point at which the (γ, α) rate becomes stronger than the (γ, n) rate for each model. The uncertainty bands correspond to the χ^2 percentage that the model combination achieved for the given reaction. The numbers in the legends refer to the LD-αOMP-γSF models used in TALYS calculations.

only the values obtained in this paper were used to determine the best-fit model. For the ^{110}Cd(α, γ) ^{114}Sn values the best-fit model was 5-5-5.

(4) The last three sentences of the second full paragraph on p. 7 should read: From this, the model combination 2-6-1 was found to be able to describe all of the data within a threshold of 60%. The combination 2-6-1 is the backshifted Fermi gas level-density (LD) model with the α-optical-model potential (αOMP) from Avrigeanu [4] and the Kopecky-Uhl generalized Lorentzian γ-ray-strength function (γSF). From this, the combination 2-6-1 is recommended for predicting cross sections within this mass range.

TABLE III. Upper portion gives χ^2 thresholds for each of the measured reactions. For details on how these thresholds were calculated see the text. The bottom portion gives the calculated χ^2 values for different model combinations. In the combination names the first number corresponds to the level-density model used, the second number is the α-optical model potential used, and the third number is the γ-strength function used.

	^{90}Zr	^{102}Pd	^{108}Cd	^{110}Cd
10%	1.42	0.38	0.97	0.19
20%	5.68	1.53	3.87	0.75
30%	12.78	3.44	8.70	1.68
50%	35.51	9.56	24.17	4.68
2-6-1	12.18	2.05	30.54	4.08
4-5-8	6.65	1548.5	128.9	116.6
5-5-4	100.4	1.58	30.6	1.15
6-4-5	295.9	65.8	9.49	4.93
5-5-5	238.6	2.79	24.8	0.29

TABLE IV. Recommended (α, γ) reaction rates for the four reactions measured. All reaction rates were calculated using the TALYS 1.9 code with the backshifted Fermi gas LD model, the αOMP from Avrigeanu [4], and the Kopecky-Uhl generalized Lorentzian γSF. The uncertainties are based upon the χ^2 percentage that the model achieves for each reaction.

	$N_A \langle \sigma v \rangle$ (cm^3 mol^{-1} s^{-1})			
T (GK)	^{90}Zr	^{102}Pd	^{108}Cd	^{110}Cd
0.3	$1.90(57) \times 10^{-47}$	$3.77(90) \times 10^{-53}$	$1.9(1.1) \times 10^{-55}$	$3.5(1.6) \times 10^{-55}$
0.4	$2.33(70) \times 10^{-40}$	$2.60(62) \times 10^{-45}$	$6.4(3.6) \times 10^{-47}$	$7.0(3.3) \times 10^{-47}$
0.5	$2.30(69) \times 10^{-35}$	$7.1(1.7) \times 10^{-40}$	$2.8(1.6) \times 10^{-41}$	$3.0(1.4) \times 10^{-41}$
0.6	$1.43(43) \times 10^{-31}$	$9.9(2.4) \times 10^{-36}$	$5.0(2.9) \times 10^{-37}$	$5.4(2.5) \times 10^{-37}$
0.7	$1.48(45) \times 10^{-28}$	$2.02(48) \times 10^{-32}$	$1.25(72) \times 10^{-33}$	$1.29(61) \times 10^{-33}$
0.8	$4.5(1.3) \times 10^{-26}$	$1.07(26) \times 10^{-29}$	$7.9(4.5) \times 10^{-31}$	$7.8(3.7) \times 10^{-31}$
0.9	$5.4(1.6) \times 10^{-24}$	$2.15(52) \times 10^{-27}$	$1.8(1.0) \times 10^{-28}$	$1.75(82) \times 10^{-28}$
1	$3.4(1.0) \times 10^{-22}$	$2.07(49) \times 10^{-25}$	$1.9(1.1) \times 10^{-26}$	$1.86(87) \times 10^{-26}$
1.5	$6.6(2.0) \times 10^{-16}$	$2.03(49) \times 10^{-18}$	$2.4(1.4) \times 10^{-19}$	$2.5(1.2) \times 10^{-19}$
2	$5.7(1.7) \times 10^{-12}$	$4.15(99) \times 10^{-14}$	$6.5(3.7) \times 10^{-15}$	$7.1(3.3) \times 10^{-15}$
2.5	$3.3(1.0) \times 10^{-9}$	$3.99(96) \times 10^{-11}$	$8.7(5.0) \times 10^{-12}$	$7.9(3.7) \times 10^{-12}$
3	$3.6(1.1) \times 10^{-7}$	$6.4(1.5) \times 10^{-9}$	$1.75(99) \times 10^{-9}$	$1.10(52) \times 10^{-9}$
3.5	$1.18(35) \times 10^{-5}$	$3.02(73) \times 10^{-7}$	$9.4(5.3) \times 10^{-8}$	$3.9(1.9) \times 10^{-8}$
4	$1.73(52) \times 10^{-4}$	$5.8(1.4) \times 10^{-6}$	$1.9(1.1) \times 10^{-6}$	$5.6(2.7) \times 10^{-7}$
5	$7.6(2.3) \times 10^{-3}$	$3.50(84) \times 10^{-4}$	$1.19(68) \times 10^{-4}$	$2.2(1.0) \times 10^{-5}$
6	$8.8(2.6) \times 10^{-2}$	$4.7(1.1) \times 10^{-3}$	$1.52(87) \times 10^{-3}$	$2.6(1.2) \times 10^{-4}$
7	$4.3(1.3) \times 10^{-1}$	$2.90(70) \times 10^{-2}$	$8.8(5.0) \times 10^{-3}$	$1.79(84) \times 10^{-3}$
8	$1.23(37) \times 10^{0}$	$1.19(29) \times 10^{-1}$	$3.5(2.0) \times 10^{-2}$	$8.7(4.1) \times 10^{-3}$
9	$2.46(75) \times 10^{0}$	$3.83(92) \times 10^{-1}$	$1.11(63) \times 10^{-1}$	$3.1(1.4) \times 10^{-2}$
10	$4.1(1.2) \times 10^{0}$	$9.6(2.3) \times 10^{-1}$	$2.8(1.6) \times 10^{-1}$	$8.0(3.8) \times 10^{-2}$

(5) The last full paragraph on p. 7 should read: Since the combination 2-6-1 is able to describe all four reactions within the 60% χ^2 threshold, this means that this combination is able to describe all of the measured cross-section values on average within a factor of 0.4–1.6.

(6) The first sentence of the last paragraph of the conclusions should read: It was determined that the combination of the backshifted Fermi gas LD model with the αOMP from Avrigeanu [4] and the Kopecky-Uhl generalized Lorentzian γSF reproduced all of the measured results within 60%.

(7) In addition, the numbering of the microscopic LD models was incorrect. For consistency with input description in Talys, the three microscopic LDs listed on page 5 should be numbered as 4,5 and 6 instead of 1,2 and 3. They should appear as:

(4) microscopic level densities calculated using a Skyrme force from Goriely's tables [5],

(5) microscopic level densities calculated using a Skyrme force from Hilaire's combinatorial tables [6], and

(6) microscopic level densities calculated using a Gogny force from Hilaire's combinatorial tables [7].

---

[1] S. J. Quinn, A. Spyrou, A. Simon, A. Battaglia, M. Bowers, B. Bucher, C. Casarella, M. Couder, P. A. DeYoung, A. C. Dombos, J. Görres, A. Kontos, Q. Li, A. Long, M. Moran, N. Paul, J. Pereira, D. Robertson, K. Smith, M. K. Smith *et al.*, Phys. Rev. C **92**, 045805 (2015).

[2] P. Scholz, F. Heim, J. Mayer, C. Münker, L. Netterdon, F. Wombacher, and A. Zilges, Phys. Lett. B **761**, 247 (2016).

[3] P. Scholz (private communication).

[4] V. Avrigeanu, M. Avrigeanu, and C. Mănăilescu, Phys. Rev. C **90**, 044612 (2014).

[5] S. Goriely, F. Tondeur, and J. Pearson, At. Data Nucl. Data Tables **77**, 311 (2001).

[6] S. Goriely, S. Hilaire, and A. J. Koning, Phys. Rev. C **78**, 064307 (2008).

[7] S. Hilaire, M. Girod, S. Goriely, and A. J. Koning, Phys. Rev. C **86**, 064317 (2012).